Protein–Protein Interactions Hot Paper

DOI: 10.1002/ange.201403773

A Natural-Product Switch for a Dynamic Protein Interface**

Marcel Scheepstra, Lidia Nieto, Anna K. H. Hirsch, Sascha Fuchs, Seppe Leysen, Chan Vinh Lam, Leslie in het Panhuis, Constant A. A. van Boeckel, Hans Wienk, Rolf Boelens, Christian Ottmann, Lech-Gustav Milroy, and Luc Brunsveld**

Abstract: *Small ligands are a powerful way to control the function of protein complexes via dynamic binding interfaces. The classic example is found in gene transcription where small ligands regulate nuclear receptor binding to coactivator proteins via the dynamic activation function 2 (AF2) interface. Current ligands target the ligand-binding pocket side of the AF2. Few ligands are known, which selectively target the coactivator side of the AF2, or which can be selectively switched from one side of the interface to the other. We use NMR spectroscopy and modeling to identify a natural product, which targets the retinoid X receptor (RXR) at both sides of the AF2. We then use chemical synthesis, cellular screening and X-ray co-crystallography to split this dual activity, leading to a potent and molecularly efficient RXR agonist, and a first-of-kind inhibitor selective for the RXR/coactivator interaction. Our findings justify future exploration of natural products at dynamic protein interfaces.*

Small ligands are a powerful way to control the function of large protein complexes via the selective modulation of dynamic binding interfaces.[1] A classic example of this is seen in eukaryotic gene transcription initiation, and the protein complex formed between nuclear receptors and coactivator proteins via the dynamic activation function 2 (AF2) binding interface.[2] Ligand binding to a hydrophobic pocket located at the solvent-excluded side of the AF2 (Scheme 1), within the nuclear receptor ligand-binding domain,[3] allosterically stabilizes or destabilizes coactivator protein binding at the opposite, solvent-exposed side of the interface, which in turn determines the transcriptional output. Ligand binding thus functions as a molecular switch, where stabilization or destabilization of the AF2 switches gene transcription either "on" or "off".[4]

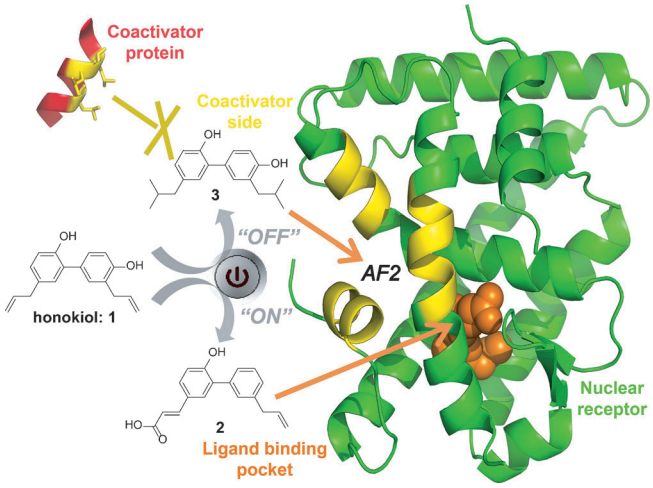

Scheme 1. Regulation of the dynamic nuclear receptor interface—the activation function 2 (AF2)—by using small synthetic ligands derived from the same natural product (**1**): stabilization of the AF2 through binding at the ligand-binding pocket (**2**); destabilization of the AF2 through binding at the coactivator side of the interface (**3**).[11]

Ligands targeting the nuclear receptor ligand-binding pocket continue to be an important source of drug molecules.[5] However, issues of toxicity and drug resistance mean that ligands with atypical modes-of-action are in urgent demand.[6] For instance, ligands targeting the ligand binding pocket but with atypical partial agonist/antagonist behavior—so-called selective nuclear receptor modulators—are less toxic due to tissue-selective behavior.[7] Alternatively, modified peptides derived from the binding epitopes of coactivator proteins or phage peptides selectively target the coactivator side of the AF2.[8] Small non-peptidic ligands[9] are arguably better suited than peptides as coactivator inhibitors due to their high ligand efficiency, metabolic stability and cell permeability, and some have shown promising NR-selective behavior.[9e,f,j] Natural products, though well investigated at

[*] M. Scheepstra, Dr. L. Nieto, Dr. S. Fuchs, Dr. S. Leysen, C. V. Lam, L. in het Panhuis, Prof. Dr. C. A. A. van Boeckel, Dr. C. Ottmann, Dr. L.-G. Milroy, Prof. Dr. L. Brunsveld
Laboratory of Chemical Biology and Institute of Complex Molecular Systems (ICMS), Department of Biomedical Engineering
Technische Universiteit Eindhoven
Den Dolech 2, 5612 AZ Eindhoven (The Netherlands)
E-mail: l.milroy@tue.nl
l.brunsveld@tue.nl
Homepage: http://www.tue.nl/cb
Dr. A. K. H. Hirsch
Stratingh Institue for Chemistry, University of Groningen
Nijenborgh 7, 9747AG Groningen (The Netherlands)
Dr. H. Wienk, Prof. Dr. R. Boelens
Bijvoet Center for Biomolecular Research, NMR Spectroscopy
Utrecht University, Padualaan 8, 3584CH Utrecht (The Netherlands)

[**] We thank Nicky Hoek, Dr. Eric Kalkhoven and Dr. Arjen Koppen (UMC, Utrecht, The Netherlands) for their scientific support. Funding was granted by the Netherlands Organisation for Scientific Research via Gravity program 024.001.035, ECHO grant 711011017, VENI grant to A.K.H.H., and a Marie Curie Action (PIEF-GA-2011-298489 to LN).

Supporting information for this article (synthesis protocols, analytical data for all novel compounds, biochemical and cellular evaluation of compounds, including cofactor recruitment, fluorescence polarization, molecular modeling, STD-NMR, CORCEMA-ST, and X-ray co-crystallography) is available on the WWW under http://dx.doi.org/10.1002/anie.201403773.

the ligand-binding pocket, have been underexplored at the coactivator-side of the AF2, and are well suited for this purpose due to their biological relevance and the unique and diverse chemical space they populate.[10]

Herein, we report the development of two different ligand types, originating from the same natural product, targeting different sides of a dynamic interface, and with opposite stabilizing/destabilizing properties. We used co-factor recruitment screening and a combination of STD-NMR spectroscopy, molecular docking, and CORCEMA-ST calculations to show that honokiol (**1**, Scheme 1) targets both sides of the AF2 of the retinoid X receptor (RXR).[12] We then applied a rational chemical-biology approach, with an efficient synthesis protocol at its core, to split the dual-binding behavior of **1** and create a potent and molecularly efficient RXR agonist and an atypical RXR-selective antagonist (**2** and **3**, Scheme 1).

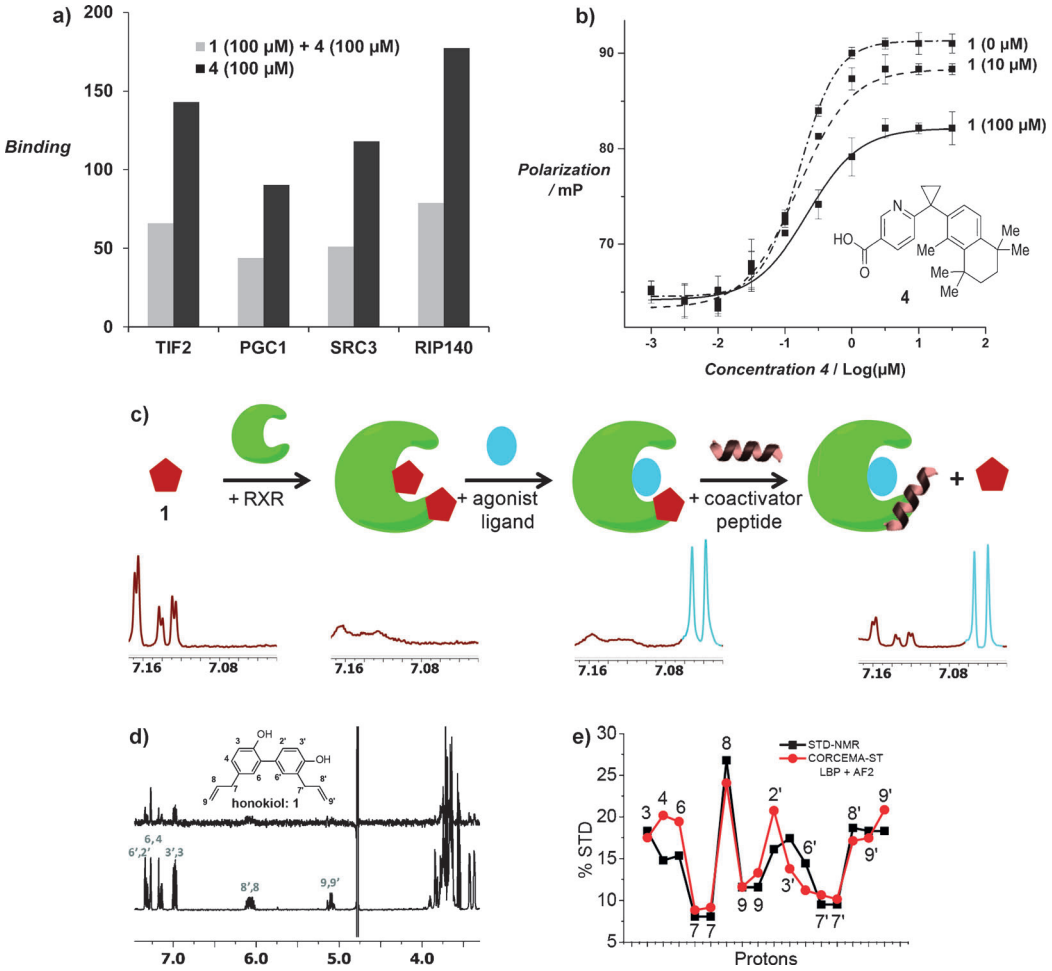

Figure 1. Honokiol (**1**) binds to both sides of the dynamic AF2 interface of RXR. a) Four selected examples from a fluorescence-based co-factor-recruitment assay showing inhibition of coactivator protein binding at 100 μM of **1** in the presence of a potent full agonist, **4**. b) Fluorescence polarization data showing that full agonist **4** induces binding of a fluorescently labeled coactivator peptide in a concentration-dependent manner. Repeating the assay in the presence of increasing concentrations of **1** (10, 100 μM) resulted in a progressive decrease in the maximum polarization signal, but without changing the EC_{50} of **4**, thus showing an alternative binding mode. c) A summary of 1D-^{1}H NMR data revealing the atypical dual binding of **1**: line broadening of the ^{1}H resonances of **1** in the presence of protein and agonist ligand; recovery of sharp intense signals on addition of a competitor LXXLL peptide; d) ^{1}H NMR spectrum of honokiol (**1**; bottom) and STD (saturation transfer difference) spectrum of the system **1**/RXR (top) show rapid ligand exchange. e) The sum of separate theoretical CORCEMA-ST[13] values at the ligand binding pocket and coactivator side of the AF2 interface compare well with the experimental STD data for the system **1**/RXR, thus indicating the dual ligand binding mode.

The RXR–coactivator interaction is important for the development of cancer,[14] metabolic disorder,[15] and Alzheimer's disease.[16] Current RXR ligands target the ligand-binding pocket, for which a rigid and bulky hydrocarbon-rich moiety is typically needed for potent binding (e.g., LG100268, **4**, Figure 1 b).[17] Non-peptidic ligands targeting the coactivator side of the RXR AF2 are at present non-existent. For these reasons we became interested in the atypical RXR activity of honokiol (**1**, Scheme 1).[18] Alongside related natural products isolated from the Magnolia tree bark,[19] **1** displays an array of biological properties, including neurite-growth induction and anti-angiogenic effects. It is likely that **1** targets multiple proteins,[20] in light of its fragment-like profile ($M_W = 266$ Da),[10,21] and because of the privileged nature of the biaryl structural motif.[22] Importantly, **1** has also shown evidence of partial activity in a luciferase-based screen using U2OS cells overexpressing RXR.[18]

We profiled the RXR-activity of **1** alongside analogous natural and synthetic biaryl ligands using a fluorescence-based co-factor-recruitment assay (Figure 1 a and Supporting Information), where an increase in fluorescence signal would correspond with ligand binding at the RXR ligand binding pocket.[23] In contrast to the other ligands tested, and contrary to our initial expectations, **1** inhibited coactivator-binding at 100 μM ligand concentration in the presence and absence of 100 μM of a potent full agonist, **4** (Figure 1 a). At 100 μM, **4** fully saturates the ligand binding pocket, and thus excludes

the binding of **1** at the ligand binding pocket. In support of this, a separate fluorescence polarization binding assay was performed, in which increasing concentrations of **4** predictably induced recruitment of a fluorescently labelled coactivator peptide (Figure 1b). Repeating the assay in the presence of increasing amounts of **1** resulted in a concentration-dependent decrease in the maximum polarization signal, but without detectable changes in the EC_{50} for **4** (Figure 1b). The K_i for **1** was determined to be 94 μM ± 9 μM (Supporting Information). This atypical behavior of **1** indicated to us a mode-of-binding distinct from the ligand binding pocket. Despite a growing number of non-peptidic coactivator inhibitor ligands,[6a,c,9] only a few are reported to be selective for one nuclear receptor over others,[9e,f,j] of which none are natural products and none selective for RXR. Importantly, therefore, we found **1** to be selective for RXR over the estrogen and androgen receptors (ER and AR) in a fluorescence-based co-factor-recruitment assay (Supporting Information). Repeating the competitive fluorescence polarization assay in the presence of detergent did not alter the binding profile (Supporting Information),[25] which, coupled with the inactivity of **1** towards ER and AR confirms the physiological significance of the interaction between **1** and RXR. In conclusion, **1** selectively inhibits the RXR–coactivator interaction in a physiologically significant manner and via an atypical mechanism, which is independent of the ligand-binding pocket.

In-depth ligand-detected NMR studies were performed to further elucidate the RXR-binding mode of **1** (Figure 1c, Supporting Information). Severe line broadening of the ^1H resonances of **1** was observed in the presence of the RXR protein, which could be explained by the moderate binding affinity of the compound, as evidenced by our fluorescence polarization data, and the rapid ligand exchange. Line broadening of **1** was also observed in the presence of protein and an excess of potent ligands **2** and **4** (Figure 1c, Supporting Information). However, signal intensity and sharpening of **1** recovered upon addition of a coactivator-derived peptide (Figure 1c), indicating competitive inhibition of **1** by the peptide. STD experiments on the system **1**/RXR revealed the rapid exchange between free and bound states (Figure 1d). These data, combined with detailed competition STD and tr-NOESY NMR experiments (Supporting Information) suggest a novel binding mode for **1** at the coactivator side of the AF2. Moreover, theoretical CORCEMA-ST[13] data show that the experimental STD data collected for the **1**/RXR system correspond with a dual ligand binding mode (Figure 1d and e, Supporting Information) at both the ligand-binding pocket and the coactivator side.

To capitalize on the dual-binding properties of **1**, we developed an orthogonal pair of RXR ligands capable of selectively targeting opposite sides of the dynamic AF2 surface. We had reason to believe that **1** inhibits coactivator-binding by mimicking the LXXLL binding motif, which is highly conserved throughout coactivator proteins. Indeed, an overlay of the energy-minimized state of **1** and the co-crystal structure of an α-helical coactivator peptide bound to RXR (PDB ID: 2P1T)[26] identified a strong overlap of the interacting Leu residues at positions *i* and *i*+4 of the α-helix and the allylic side-chains of **1** (Figure 2a). Furthermore, the 4′-hydroxy functional group (*para* to the biaryl bond) makes a stabilizing hydrogen-bonding interaction with Glu453—a charge-clamp residue important for selective binding of the helical LXXLL motif—on molecular docking of the LXXLL-aligned model of **1** to the AF2.

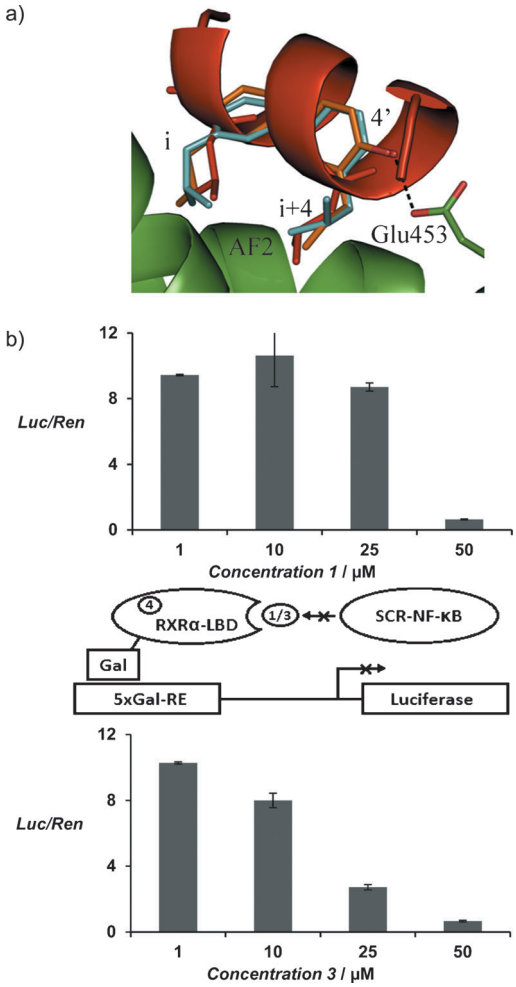

Figure 2. a) Overlay of honokiol (**1**; orange) and LXXLL mimic **3** (cyan) with the LXXLL-coactivator peptide (red, PDB ID: 2P1T) bound to the RXR AF2.[26] b) Cellular activities of **1** and **3** measured in a mammalian two-hybrid luciferase assay in which increasing concentrations of the ligand are co-incubated with a fixed, 100 nM, concentration of full RXR agonist, **4**.

To favor selective AF2 binding, we synthesized isobutyl analog **3** (Scheme 1; 25%, 3 steps, Supporting Information), which we initially hypothesized would serve as a better mimic than **1** of the LXXLL motif. Experimentally, analog **3** was inactive as agonist in a mammalian two-hybrid assay (M2H) up to 50 μM (Table 1). In the same agonistic assay, however, **1** alone elicited a complex response, which we explain by the dual binding properties delineated in Figure 1c–e. Although an EC_{50} value could not be determined for **1** in this case, nevertheless at concentrations between 1–25 μM, **1** induced partial activation of luciferase expression followed by inhibition at the highest 50 μM test concentration.[18a] The catalytic activity of the luciferase protein was unchanged, in the

Table 1: Summary of fluorescence polarization (FP) and mammalian two-hybrid (M2H) data for synthetic ligands vs. honokiol (**1**) and LG 100268 (**4**).[a]

Compound[b]	FP/EC_{50} [μM][c]	M2H (Luciferase)/EC_{50} [μM][d]
LG100268 (**4**)	0.15 ± 0.04	0.0051 ± 0.002
1	inactive	–[e]
2	0.26 ± 0.11	0.0063 ± 0.004
3	inactive	inactive
15	>250	>50
17	>250	>50
18	8.3 ± 2.2	0.31 ± 0.04
19	1.2 ± 0.48	6.2 ± 1.6

[a] Please refer to Supporting Information for activity curves. [b] See Figure 3 for further synthesis details. [c] Fluorescence polarization (FP) assay to determine direct binding (EC_{50}). [d] Agonistic mammalian two-hybrid (M2H) luciferase assay (EC_{50}). See the Supporting Information for details about the different assay formats. [e] Partial activity measured, see Supporting Information and reference [18a].

absence or presence of **1** and **3** (Supporting Information), thus ruling out direct inhibition of luciferase as a possible mode-of-action. Similar to **1**, analog **3** also inhibited coactivator binding to the AF2 in the fluorescence polarization assay, albeit with slightly reduced affinity ($K_i = 199 \pm 2$ μM). Importantly though, analog **3** was more effective than **1** at suppressing the full agonistic activity of **4** in the mammalian two-hybrid assay (Figure 2b). The improved cellular activity of **3** can be explained by an improved selectivity for the solvent-exposed coactivator side of the AF2. Indeed molecular modeling suggested that the isobutyl substituents on **3** disfavor binding at the ligand binding pocket due to additional repulsive interactions (Supporting Information). We conclude therefore that compared to **1**, LXXLL mimic **3** selectively inhibits the RXR–coactivator interaction via a more preferential binding at the coactivator side of the dynamic AF2 interface.

Our next aim was to switch selectivity from the coactivator side of the AF2 to the ligand-binding pocket. Potent RXR ligands targeting the ligand-binding pocket (e.g., **4**, Figure 1b) typically require a carboxylate group, which forms a salt-bridge with residue Arg116 in the hydrophilic region of the binding pocket. Our modeling data (Supporting Information) indicated that modifying one of the allylic side-chains of **1** to a carboxylate group would favor binding at the ligand-binding pocket. Unsure of the binding preference, we synthesized analogs **15**, **17**, and **18** using an efficient palladium-catalyzed cross-coupling route (Figure 3 and Supporting Information) in which the key biaryl bond was formed under Buchwald-modified Suzuki conditions.[27] Whereas **15** and **17** were only weakly active in both fluorescence polarization and M2H assays, analog **18** showed significant activity ($EC_{50(FP)} = 8.3 \pm 2.2$ μM; $EC_{50(M2H)} = 0.31 \pm 0.04$ μM, Table 1). Our binding model hinted at further activity gains by removing the 4′-hydroxy group (Figure 3, $R^2 = OH \rightarrow H$). Therefore, analog **2** (Scheme 1 and Figure 3) was prepared via a similar synthetic route, and, was gratifyingly 40-fold more active than **18** ($EC_{50(FP)} = 0.26 \pm 0.06$ μM; $EC_{50(M2H)} = 0.063 \pm 0.004$ μM, Table 1). The 20- to 30-fold difference between the FP and M2H data is a common phenomemon,[9k] which can be explained by intrinsic differences between the two different assay formats, in particular, the different protein and peptide concentrations used.

To gain further molecular insight at the ligand-binding pocket, the X-ray co-crystal of **2** bound to the RXR ligand-binding domain was solved at 2.6 Å resolution (Figure 4). The carboxylate group of **2** is seen making a canonical interaction with Arg116, while the flexible allylic side-chain occupies the lipophilic region of the binding pocket. A molecular overlay with known RXR co-crystal structures (PDB IDs: 2P1T and 4K6I) did not reveal any significant differences in global protein conformation. We could not find electron density in the X-ray structure, nor evidence from MS data (Supporting Information) to suggest covalent attachment of **2** to the RXR protein, thus ruling out irreversible inhibition as a possible mode-of-action. Combined with the biochemical and cellular results, this data suggests that, in contrast to current RXR

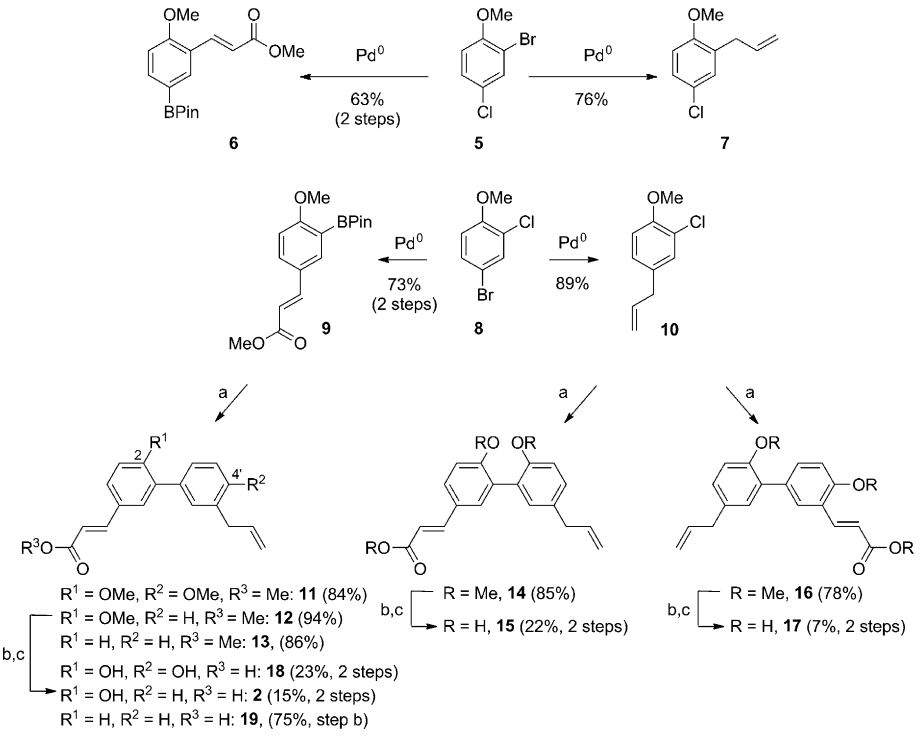

Figure 3. Synthesis of ligands targeting the ligand-binding pocket. Reagents and conditions: a) [$Pd_2(dba)_3$], SPhos, 1,4-dioxane/H_2O, 110°C, 18 h; b) aq. NaOH; c) BBr_3. Details see Supporting Information.

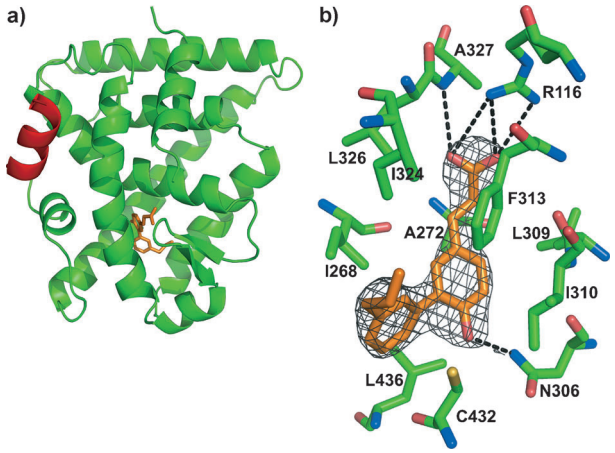

Figure 4. Ribbon representation of the X-ray co-crystal structure (PDB ID: 4OC7) of **2** bound to the RXR ligand-binding domain: a) protein (green), TIF2-derived coactiavator peptide (red), **2** (orange). b) Zoomed-in view of the RXR ligand-binding pocket with amino acid side-chains represented as sticks, and the electron density map of **2**.

ligands, a rigid and bulky hydrophobic moiety is not necessary for potent binding at the ligand-binding pocket. However, analog **19** lacking the hydroxy groups at the 2- and 4′-positions (Figure 3) was significantly less active than **2** (> 200-fold), highlighting the importance of the 2-hydroxy group for activity,[26] by simultaneously restricting the rotational freedom about the biaryl bond and through formation of a hydrogen-bonding interaction with residue Asn306. Thus, by rational design and using a short and focused synthetic route, we managed a selective switch of the targeting properties of **1** from one side of the dynamic AF2 interface of RXR to the other—from the solvent-exposed side to the ligand-binding pocket—and most notably with improved ligand efficiency (BEI)[24] compared to known RXR ligands (**2**, $BEI_{(FP)} = 23.5$ vs. **4**, $BEI_{(FP)} = 18.8$).

In summary, we demonstrate the rational splitting of the dual-binding properties of a natural product at a dynamic protein interface. This outcome has resulted in two distinct and molecularly efficient ligand types targeting opposite sides of the activation function 2 (AF2) of the retinoid X receptor (RXR). The first ligand type, represented by **3**, exhibits an atypical behavior, inhibiting coactivator binding at the solvent-exposed side of the AF2 interface. Notably, ligand **3** is the first of its kind selective for RXR. The second type, represented by **2**, potently binds to the ligand-binding pocket, thereby inducing coactivator binding via an established mechanism. Our findings justify the future exploration of natural products at dynamic protein interfaces.

Received: March 27, 2014
Published online: May 12, 2014

Keywords: drug discovery · natural products · nuclear receptors · protein–protein interactions · retinoid X receptor

[1] a) C. Y. Majmudar, J. W. Højfeldt, C. J. Arevang, W. C. Pomerantz, J. K. Gagnon, P. J. Schultz, L. C. Cesa, C. H. Doss, S. P. Rowe, V. Vásquez, et al., *Angew. Chem.* **2012**, *124*, 11420 – 11424; *Angew. Chem. Int. Ed.* **2012**, *51*, 11258 – 11262; b) N. Wang, C. Y. Majmudar, W. C. Pomerantz, J. K. Gagnon, J. D. Sadowsky, J. L. Meagher, T. K. Johnson, J. A. Stuckey, C. L. Brooks, J. A. Wells, A. K. Mapp, *J. Am. Chem. Soc.* **2013**, *135*, 3363 – 3366.
[2] P. Huang, V. Chandra, F. Rastinejad, *Annu. Rev. Physiol.* **2010**, *72*, 247 – 272.
[3] J.-M. Wurtz, W. Bourguet, J.-P. Renaud, V. Vivat, P. Chambon, D. Moras, H. Gronemeyer, *Nat. Struct. Mol. Biol.* **1996**, *3*, 87 – 94.
[4] L. Nagy, J. W. R. Schwabe, *Trends Biochem. Sci.* **2004**, *29*, 317 – 324.
[5] a) J. T. Moore, J. L. Collins, K. H. Pearce, *ChemMedChem* **2006**, *1*, 504 – 523.
[6] a) T. W. Moore, C. G. Mayne, J. A. Katzenellenbogen, *Mol. Endocrinol.* **2010**, *24*, 683 – 695; b) J. H. Choi, A. S. Banks, T. M. Kamenecka, S. A. Busby, M. J. Chalmers, N. Kumar, D. S. Kuruvilla, Y. Shin, Y. He, J. B. Bruning, et al., *Nature* **2011**, *477*, 477 – 481; c) P. Sadana, *Future Med. Chem.* **2012**, *4*, 1307 – 1333.
[7] C. L. Smith, B. W. O'Malley, *Endocr. Rev.* **2004**, *25*, 45 – 71.
[8] a) T. R. Geistlinger, R. K. Guy, *J. Am. Chem. Soc.* **2003**, *125*, 6852 – 6853; b) C. Phillips, L. R. Roberts, M. Schade, R. Bazin, A. Bent, N. L. Davies, R. Moore, A. D. Pannifer, A. R. Pickford, S. H. Prior, et al., *J. Am. Chem. Soc.* **2011**, *133*, 9696 – 9699.
[9] a) V. Azzarito, K. Long, N. S. Murphy, A. J. Wilson, *Nat. Chem.* **2013**, *5*, 161 – 173; b) L. A. Arnold, E. Estébanez-Perpiñá, M. Togashi, N. Jouravel, A. Shelat, A. C. McReynolds, E. Mar, P. Nguyen, J. D. Baxter, R. J. Fletterick, et al., *J. Biol. Chem.* **2005**, *280*, 43048 – 43055; c) L. A. Arnold, A. Kosinski, E. Estébanez-Perpiñá, R. J. Fletterick, R. K. Guy, *J. Med. Chem.* **2007**, *50*, 5269 – 5280; d) J. Becerril, A. D. Hamilton, *Angew. Chem.* **2007**, *119*, 4555 – 4557; *Angew. Chem. Int. Ed.* **2007**, *46*, 4471 – 4473; e) J. R. Gunther, A. A. Parent, J. A. Katzenellenbogen, *ACS Chem. Biol.* **2009**, *4*, 435 – 440; f) P. Nandhikonda, W. Z. Lynt, M. M. McCallum, T. Ara, A. M. Baranowski, N. Y. Yuan, D. Pearson, D. D. Bikle, R. K. Guy, L. A. Arnold, *J. Med. Chem.* **2012**, *55*, 4640 – 4651; g) A. L. Rodriguez, A. Tamrazi, M. L. Collins, J. A. Katzenellenbogen, *J. Med. Chem.* **2004**, *47*, 600 – 611; h) E. Estébanez-Perpiñá, L. A. Arnold, A. A. Arnold, P. Nguyen, E. D. Rodrigues, E. Mar, R. Bateman, P. Pallai, K. M. Shokat, J. D. Baxter, et al., *Proc. Natl. Acad. Sci. USA* **2007**, *104*, 16074 – 16079; i) A. Sun, T. W. Moore, J. R. Gunther, M.-S. Kim, E. Rhoden, Y. Du, H. Fu, J. P. Snyder, J. A. Katzenellenbogen, *ChemMedChem* **2011**, *6*, 654 – 666; j) L. Caboni, G. K. Kinsella, F. Blanco, D. Fayne, W. N. Jagoe, M. Carr, D. C. Williams, M. J. Meegan, D. G. Lloyd, *J. Med. Chem.* **2012**, *55*, 1635 – 1644; k) A. L. LaFrate, J. R. Gunther, K. E. Carlson, J. A. Katzenellenbogen, *Bioorg. Med. Chem.* **2008**, *16*, 10075 – 10084.
[10] B. Over, S. Wetzel, C. Grütter, Y. Nakai, S. Renner, D. Rauh, H. Waldmann, *Nat. Chem.* **2013**, *5*, 21 – 28.
[11] The PyMOL Molecular Graphics System, Version 1.5.0.4 Schrödinger, LLC.
[12] A. R. de Lera, W. Bourguet, L. Altucci, H. Gronemeyer, *Nat. Rev. Drug Discovery* **2007**, *6*, 811 – 820.
[13] a) V. Jayalakshmi, N. R. Krishna, *J. Magn. Reson.* **2002**, *155*, 106 – 118; b) N. R. Krishna, V. Jayalakshmi, *Top. Curr. Chem.* **2008**, *273*, 15 – 54.
[14] K. T. Liby, M. M. Yore, M. B. Sporn, *Nat. Rev. Cancer* **2007**, *7*, 357 – 369.
[15] L. Altucci, M. D. Leibowitz, K. M. Ogilvie, A. R. de Lera, H. Gronemeyer, *Nat. Rev. Drug Discovery* **2007**, *6*, 793 – 810.

[16] P. E. Cramer, J. R. Cirrito, D. W. Wesson, C. Y. D. Lee, J. C. Karlo, A. E. Zinn, B. T. Casali, J. L. Restivo, W. D. Goebel, M. J. James, et al., *Science* **2012**, *335*, 1503 – 1506.
[17] J. H. Barnard, J. C. Collings, A. Whiting, S. A. Przyborski, T. B. Marder, *Chem. Eur. J.* **2009**, *15*, 11430 – 11442.
[18] a) H. Kotani, H. Tanabe, H. Mizukami, M. Makishima, M. Inoue, *J. Nat. Prod.* **2010**, *73*, 1332 – 1336; b) C.-G. Jung, H. Horike, B.-Y. Cha, K.-O. Uhm, R. Yamauchi, T. Yamaguchi, T. Hosono, K. Iida, J.-T. Woo, M. Michikawa, *Biol. Pharm. Bull.* **2010**, *33*, 1105 – 1111.
[19] Y.-J. Lee, Y. M. Lee, C.-K. Lee, J. K. Jung, S. B. Han, J. T. Hong, *Pharmacol. Ther.* **2011**, *130*, 157 – 176.
[20] a) P. Banerjee, A. Basu, J. L. Arbiser, S. Pal, *Cancer Lett.* **2013**, *338*, 292 – 299; b) T. Singh, S. K. Katiyar, *PLoS ONE* **2013**, *8*, e60749; c) A. Kumar, U. Kumar Singh, A. Chaudhary, *Future Med. Chem.* **2013**, *5*, 809 – 829.
[21] C. W. Murray, D. C. Rees, *Nat. Chem.* **2009**, *1*, 187 – 192.
[22] D. A. Horton, G. T. Bourne, M. L. Smythe, *Chem. Rev.* **2003**, *103*, 893 – 930.
[23] A. Koppen, R. Houtman, D. Pijnenburg, E. H. Jeninga, R. Ruijtenbeek, E. Kalkhoven, *Mol. Cell. Proteomics* **2009**, *8*, 2212 – 2226.
[24] C. Abad-Zapatero, *Expert Opin. Drug Discovery* **2007**, *2*, 469 – 488.
[25] B. Y. Feng, B. K. Shoichet, *Nat. Protoc.* **2006**, *1*, 550 – 553.
[26] V. Nahoum, E. Pérez, P. Germain, F. Rodríguez-Barrios, F. Manzo, S. Kammerer, G. Lemaire, O. Hirsch, C. A. Royer, H. Gronemeyer, et al., *Proc. Natl. Acad. Sci. USA* **2007**, *104*, 17323 – 17328.
[27] K. L. Billingsley, T. E. Barder, S. L. Buchwald, *Angew. Chem.* **2007**, *119*, 5455 – 5459; *Angew. Chem. Int. Ed.* **2007**, *46*, 5359 – 5363.

